



## Properties of SBR Compound using Silica-graphite Dual Phase Filler

Ji Hang Shin, A.M. Shanmugaraj, Pyoung Chan Lee\*, Sun Kyung Jeoung\*, and Sung Hun Ryu†

Department of Chemical Engineering College of Engineering Kyung Hee University and

\*Lightweight & Convergent Materials R&D Center Korea Automotive Technology Institute

(Received February 17, 2014, Revised February 21, 2014, Accepted February 25, 2014)

## 실리카-그래파이트 이원 충전제를 이용한 SBR 컴파운드의 성질

신지항 · A.M. Shanmugaraj · 이평찬\* · 정선경\* · 류승훈†

경희대학교 화학공학과

\*자동차부품연구원 경량화 융합소재 연구센터

접수일(2014년 2월 17일), 수정일(2014년 2월 21일), 게재확정일(2014년 2월 25일)

**ABSTRACT** : Carbon coating on silica particles is done by grafting expanded graphite on the silica aggregates. Successful coating of carbon is corroborated using FT-IR, TGA, XPS and TEM. Crystalline nature of coated graphite is corroborated using XRD. Influence of carbon coated silica particles on rheometric and mechanical properties of SBR composites are investigated. Carbon coated silica particles showed significant improvement in rheometric and mechanical properties, when compared to pristine silica filled system corroborating higher polymer-filler adhesion. This fact was further supported by bound rubber content and equilibrium swelling ratios of unvulcanized and vulcanized SBR composites.

**요약** : 실리카 입자에 팽창흑연을 그래프트 시킴으로 카본코팅을 실시하였으며, 이를 확인하기 위하여 FT-IR, TGA, XPS 그리고 TEM 분석을 실시하였다. 코팅된 흑연의 결정특성은 XRD를 이용하여 확인하였으며, 카본 코팅된 실리카가 SBR 컴파운드의 유변학적 그리고 기계적 성질에 미치는 영향에 대하여 살펴보았다. 카본 코팅된 실리카를 이용한 경우 순수 실리카를 이용한 경우에 비하여 SBR 컴파운드의 유변학적 그리고 기계적 성질이 크게 향상됨을 알 수 있었다. 이러한 현상은 평형팽창비율과 bound 고무 양 변화로도 확인 할 수 있었다.

**Keywords** : silica, graphite, graft, SBR, filler

### I. Introduction

Tire is important design and spring element of the vehicles and it is the most prominent rubber article regarding volume and importance. Tire consists of materials made up of long chain macromolecules and reinforcing materials that provide stiffness to the tire.<sup>1</sup>

A good pneumatic tire should (a) generate high possible traction force between the road and tire, (b) have exact steering characteristics and be predictable under all handling situations, (c) have low possible rolling resistance, and (d) give high mileage. To achieve these requirements, elastomer composites used to tire design should have excellent tensile properties, dynamic mechanical properties, excellent abrasion resistance, good fatigue and aging resistance.<sup>2</sup>

The introduction of carbon black as a reinforcing agent in 1904 lead to strongly increased tread wear resistance. Most commonly carbon black is used as reinforcing materials that

normally provides or enhances good physical properties in the cured elastomeric compounds for tire formulations. In tire treads the previously used zinc oxide was replaced by a high loading of carbon black to develop adequate physical properties, while a small amount of zinc oxide is still added because it is necessary for the curing reaction. Though the carbon black filled elastomeric composites meets the material demands for tire formulations, these systems has some serious drawbacks like higher rolling resistance and lower wet grip resistance.<sup>1</sup>

A major problem facing tire designers was the compromise between low rolling resistance, high wet grip and high wear resistance. Rolling resistance is the amount of energy a tire absorbs as it revolves and deflects. The lower the rolling resistance the less fuel is required to propel the vehicle forward. Lowering the rolling resistance, however, common results in a reduction in wet grip performance, which is unacceptable.<sup>1</sup> A major step in solving this problem can be achieved by the replacement of (part or all) carbon black by silica in the tire's tread compound. Alternatively, since the early 1940s, the carbon black has been complemented

† Corresponding Author. E-mail: shryu@khu.ac.kr

by the group of highly active silica particles to lower the rolling resistance and improve the wet grip resistance in tires.

Loading of silica as reinforcing filler in elastomeric compounds significantly lowers the rolling resistance (approximately 20 % reduction), which is the major criteria for better tire performance. The use of silica can also improve wet skid performance. By using silica fillers in their winter tires, wet skid performance increases as much as 15 %.

However, the problem associated with silica filled system is the poor abrasion resistance and tensile properties, which are key issues that affects the excellent tire performance. Lowering of tensile or abrasion properties are attributed to the filler-filler aggregation in non-polar matrix such as SBR.<sup>3</sup> To overcome these problem, certain coupling agents are used to reduce the filler-filler aggregation and improve the polymer-filler adhesion and tire performance.<sup>4-7</sup> Though this conventional system showed better performance, these values are far below, when compared to conventional carbon black loaded elastomeric composite based tires.

For the optimal tire performance, it is necessary to have combined properties exhibited by both carbon and silica filled elastomer system. To achieve these desired goal, carbon black companies produced a new type of fillers, which consists of carbon and silica phases (often termed as dual phase filler).<sup>8,9</sup> This filler was first developed by Cabot Corporation in late 1990's using carbon as well as silica based feedstock's.<sup>8</sup> However, these fillers doesn't show improvement in properties, when compared to carbon black system, though it showed better performance compared to silica filled elastomeric systems. Later surface coating technology was adopted by few carbon black companies, where the carbon particles are coated with silica shell.<sup>10</sup> Though it has better performance in tire formulations, the improvement in dynamic mechanical properties such as lowering of rolling resistance are not quite significant, when compared to silica filled elastomeric composites.<sup>10</sup>

In the present research, we adopt another coating technology, where silica particles are coated with carbon shell. It is expected that coating of carbon shell on silica improves the polymer-filler adhesion with non-polar polymers such as NR or SBR, which in turn improves the mechanical and physical properties such as tensile, abrasion resistance etc., quite similar to carbon black filled composites. Alternatively, silica core particles present inside the carbon shell lower the rolling resistance as well as improve the wet grip resistance, when loaded in elastomeric composites as quite relevant to silica filled elastomeric systems.

## I . Experimental

### 1. Materials and synthesis of silica grafted graphite (Silica-G)

Silica particles were coated with carbon based materials,

which were crystalline in nature. For this purpose, expanded graphite consisting of few functional active sites was selected. This coating technology was carried out by two step process. In the first step, 100 g of silica powder (SiO<sub>2</sub>, particle size 10~20 nm, Sigma Aldrich, Korea) was dispersed in 5 L of ethanol and then 3 mL of isocyanato propyl triethoxysilane (Sigma Aldrich, Korea) was added. Reaction was carried out for 24 hrs at 50°C. The resultant samples were filtered and dried under vacuum at ambient temperature. In the second step, 100 g of the silane grafted silica sample was dispersed with 50 g of expanded graphite in ethanol solvent in the presence of 10 mL of ammonium hydroxide solution (NH<sub>4</sub>OH). The processing temperature and time were optimized as 90° C and 24 hrs for the second step.

### 2. Preparation of SBR composite

Pristine and modified silica samples were loaded in solution styrene-butadiene rubber (SSBR, Buna VSL 5025-2, Lanxess) to understand their reinforcing effect. The rubber compounding formulation used in this study is depicted in Table 1.

The rubber compounds according to the formulation were prepared in open two roll mill (set with nip gap of 1:1.4 mm). The sample codes of prepared rubber compounds were designated as SBR-Filler-loading amount. For instance, SBR-SiG-10 depicts SBR composites loaded with 10 phr modified silica (Silica-G).

### 3. Characterizations

To understand the nature of interaction between the silica core and carbon shell of Silica-G, Fourier transform infrared spectroscopic (FT-IR) characterization was used. About 0.1 mg of samples were mixed with 100 mg of KBr and made into pellets. FT-IR characterization has been carried out in the range of 4000-400 cm<sup>-1</sup> using Perkin-Elmer spectrophotometer. To corroborate the crystalline nature of coated carbon in silica nanoparticles, powder X-ray diffraction studies was carried out in the 2 $\theta$  range of 5 to 50° using Macscience X-ray diffractometer (M18XHF-SRA). To understand the amount of coated carbon on silica particles, TGA characterization of silica samples were conducted in the temperature range of 25 to 700°C

**Table 1. Compounding formulation**

| Ingredient        | phr  |
|-------------------|------|
| SSBR              | 100  |
| ZnO               | 5.0  |
| Stearic acid      | 2.0  |
| Antioxidant (TMQ) | 1.0  |
| Silica filler     | 0-20 |
| MBTS              | 1.0  |
| TMTD              | 0.5  |
| Sulfur            | 2.0  |

\* MBTS: Dibenzo-thiazyl disulfide (Vulkacit DM/C, Lanxess)

\* TMTD: Tetramethyl thiuram disulfide (Vulkacit I, Lanxess)

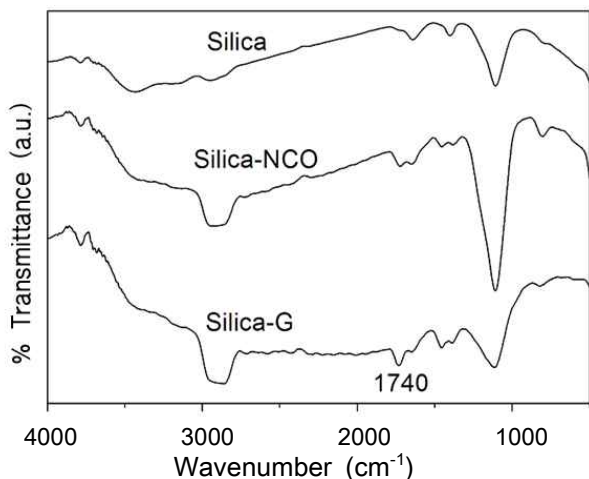


**Figure 1.** FT-IR spectra of silica, silica-NCO and silica-G

under air atmosphere at a heating rate of 10°C/min using Thermal analyzer (TA instruments, TGA Q5000 IR/SDT Q600)

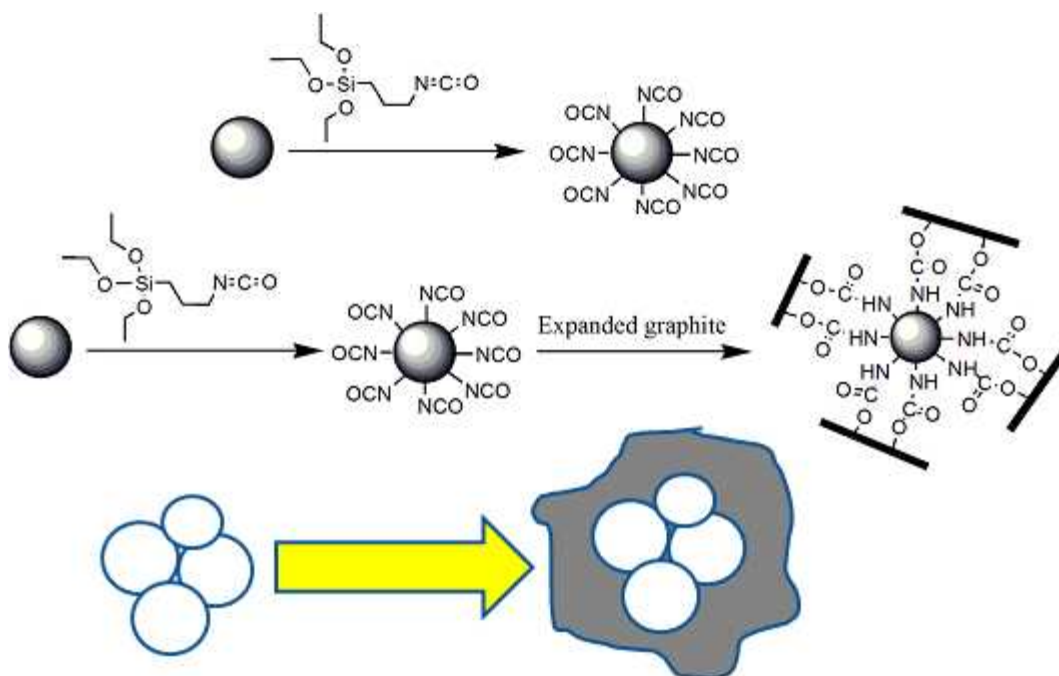
## II. Results and Discussion

Figure 1 shows the FT-IR spectra of various silicas. Pristine silica powder shows a major peak at 1100 cm<sup>-1</sup> corresponding to Si-O stretching of Si-O-Si group. Broad peak at around 3400 cm<sup>-1</sup> along with a small peak at around 1640 cm<sup>-1</sup> corroborates the -OH stretching and bending vibrations of adsorbed water molecules on the silica surface. Silane functionalization

of silica particles results in a broad peak at around 2800–3000 cm<sup>-1</sup>, attributed to -CH asymmetric and symmetric stretching corroborating the successful coating of silanes on the silica surface. These facts are corresponding further corroborated from the significant rise in peak intensity at 1100 cm<sup>-1</sup> (Si-O-Si stretching) with drastic decrease in peak at 1640 cm<sup>-1</sup> (-OH bending vibration) along with the appearance of new peak at 1450 cm<sup>-1</sup> that corresponds to the -CH bending vibration in -CH<sub>2</sub> group. Appearance of new small peak at around 2285 cm<sup>-1</sup> (-NCO groups) further reveals the successful coating of isocyanato propyl triethoxysilyl group on the silica surface.

Significant rise in peak intensity at 1740 cm<sup>-1</sup> along with the complete disappearance of peak at 2285 cm<sup>-1</sup> (-NCO groups) for Silica-G samples revealed the formation of urethane linkages, that corroborates the formation of graphite coverage on silica aggregates. Schematic representation of silica aggregates coated with expanded graphite is shown in Figure 2.

X-ray diffraction results of pristine (Si), silane functionalized (Si-NCO) and expanded graphite covered silica aggregates (Silica-G) are displayed in Figure 3. Pristine silica (Si) showed two broad peaks at 14° and 30° corroborating its amorphous nature. Silica-NCO retains the amorphous nature with the appearance of single broad peak at 21.4°. However, silica-G showed a sharp peak at 26.6° (002 peak of graphite crystals) along with a small hump at 21° (amorphous peak of Si-NCO) revealing the successful coating of expanded graphite on the silica surface. The average d-spacing values of graphite crystals grafted onto silica particles is observed at 3.35 Å.



**Figure 2.** Schematic representation of expanded graphite coated silica aggregates.

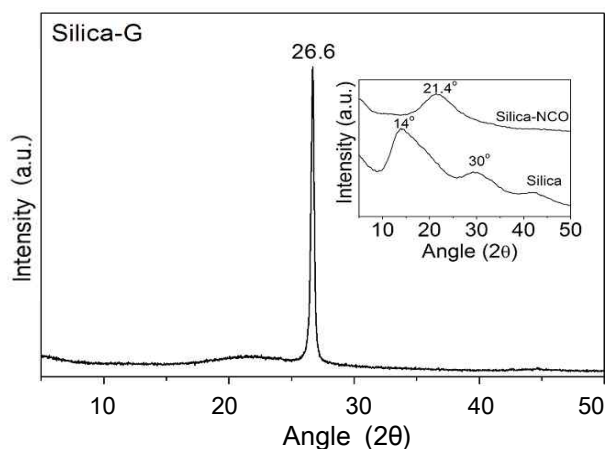


**Figure 3.** XRD results of Silica-G (inset: pristine and silane coated silica)

Thermal stability of pristine (Si), silane functionalized (Si-NCO) and expanded graphite covered silica aggregates (Silica-G) are shown in Figure 4. Pristine silica doesn't exhibit any major degradation in the selected temperature range. However, grafting of silane (Silica-NCO) showed a major weight loss (~12 %) in the temperature range of 150 to 300°C corresponding to the thermal degradation of the grafted silane

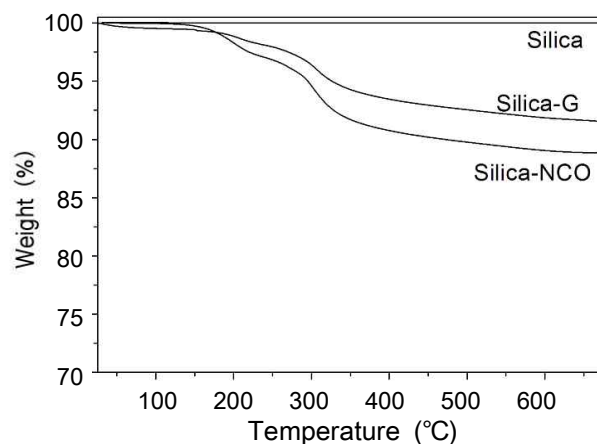


**Figure 4.** TGA thermograms of silica, silica-NCO and silica-G

molecules. Surface coverage of expanded graphite in silica particles (Silica-G) resulted in the lower degradation (~7.5 %) compared to silanized silica (Si-NCO) and it can be attributed to its thermal stability due to its crystalline nature of graphite.

Successful coating of expanded graphite on silica surfaces are further corroborated using transmission electron microscopy (TEM). About 0.1 mg of both pristine and modified silica

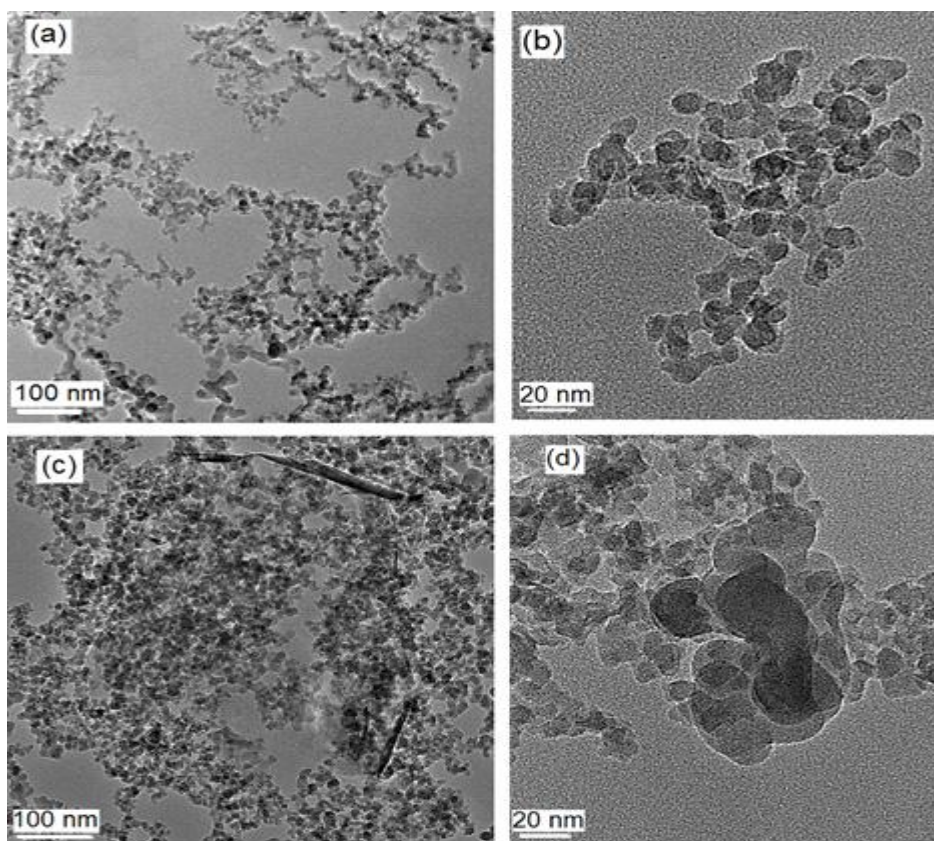


**Figure 5.** TEM images of pristine silica (a & b) and expanded graphite coated silica aggregates (c & d) at two different magnifications

(Silica-G) is dispersed in 10 mL of ethanol by ultrasonication. Few drops of dispersed samples were casted onto copper grids and subjected to morphological characterization using JEOL TEM (JEM-2100F). Figure 5 showed TEM results of pristine, graphite coated silica aggregates at lower (100 nm) and higher magnification (20 nm). Presence of thin graphene layer on the aggregated silica particle (Figure 5 c) corroborates the successful coating on the silica aggregates in case of graphite grafted silica samples (Silica-G). This fact is further revealed from the high magnification image of modified silica sample (Figure 5 d).

The surface area of the pristine silica, graphite (silica-G) coated silica aggregates were determined using BET surface area measurements (BELSORP-max) and the results are tabulated in Table 2. Grafting of graphite onto silica aggregates (Silica-G) results in 31 % decrease in BET surface area and 214 % rise in pore size. Decrease in surface area and increase in pore size is corroborated to the coating of graphene layers onto silica aggregates that reduces the nitrogen adsorption concentration onto silica aggregates.

Polymer-filler interaction is usually correlated by the presence of insoluble rubber fraction present around the silica particles, which is often termed as bound rubber content. To determine the bound rubber content in these silica filled SBR system, masterbatches (without accelerator and sulfur loading) were prepared as per the compounding formulation (Table 2). Bound rubber content was measured by dissolving 2 g of SBR masterbatches in 20 mL toluene and kept it in idle condition for 7 days. The toluene was replaced on every 2 days during the course of bound rubber studies. Bound rubber content was

**Table 2. Surface area and pore size values of pristine and graphite coated silica samples**

| S. No | Samples                        | BET surface area (m <sup>2</sup> /g) | Pore size (nm) |
|-------|--------------------------------|--------------------------------------|----------------|
| 1.    | Silica                         | 183.6                                | 7.6            |
| 2.    | Silanized silica               | 184.3                                | 14.9           |
| 3.    | Graphite grafted silica (Si-G) | 126.3                                | 23.9           |

**Table 3. Bound rubber content of silica filled SBR composites**

| S. No | Samples    | Bound rubber content (%) |
|-------|------------|--------------------------|
| 1.    | SBR0       | 1.2                      |
| 2.    | SBR-Si-10  | 8.0                      |
| 3.    | SBR-SSi-10 | 10.0                     |
| 4.    | SBR-SiG-10 | 16.0                     |
| 5.    | SBR-Si-20  | 15.0                     |
| 6.    | SBR-SiG-20 | 22.0                     |

determined from the weight loss of the samples by using the equation (1) as shown below

$$R_a(\%) = 100 \times \frac{\left[ W_{tg} - W_1 \left[ \frac{m_f}{(m_f + m_r)} \right] \right]}{W_1 \left[ \frac{m_r}{(m_r + m_f)} \right]} \quad (1)$$

Where  $W_{tg}$  is the weight of filler and gel,  $W_1$  is the weight of the sample,  $m_f$  is the fraction of rubber in the compound,  $m_r$  is the fraction of filler in the compound. Bound rubber content measured for representative samples using equation (1) is shown in Table 3. Significant rise in bound rubber content (insoluble rubber fraction) for silica-G and silica-AC filled SBR sample corroborates higher polymer-filler adhesion in this system.

The cure characteristics such as minimum torque ( $M_L$ ), maximum torque ( $M_H$ ), torque difference (DS), scorch time ( $t_{S2}$ ) and optimum cure time ( $t_{90}$ ) of the prepared rubber compounds (loaded with accelerator and sulfur) were determined using oscillating disk rheometer (ODR) measurements and the results are tabulated in Table 4. Compared to the pristine silica loaded SBR composites, modified silica filled SBR system showed lower  $M_L$  corroborating the decrease in filler-filler aggregation in SBR matrix. This effect is more pronounced on increasing the loading amount (Table 4). The torque difference, DS, which is the indirect measure of interfacial adhesion between the filler and elastomer increases for modified silica corroborating the enhanced polymer-filler interaction. Scorch time and optimum cure time of the modified silica filled SBR composites decreases revealing its accelerating effect on curing reactions.

The prepared rubber compounds were vulcanized using  $t_{90}$  values in hot press (Carvar press), set at the temperature 150°C. Tensile dumbbell samples were cut using the vulcanized samples in ASTM Die C and mechanical properties were determined using universal tensile testing machine (Instron UTM) as per ASTM standard (ASTM D 412) and the values are tabulated in Table 5. Figure 6 showed the representative stress-strain results of gum and silica filled SBR vulcanizates. Compared to pristine silica filled SBR samples, modified silica filled samples showed a significant improvement in mechanical properties such as modulus and tensile strength corroborating the reinforcing effect of the prepared modified silica samples.

Equilibrium swelling studies is generally adopted to understand the reinforcing effect of filler loaded elastomer vulcanizates. Equilibrium swelling ratio ( $Q_f$ ) is calculated by storing the cured pre-weighed SBR circular specimens in toluene solvent for about 36 hrs. The swelled samples were then re-weighed and the ratio

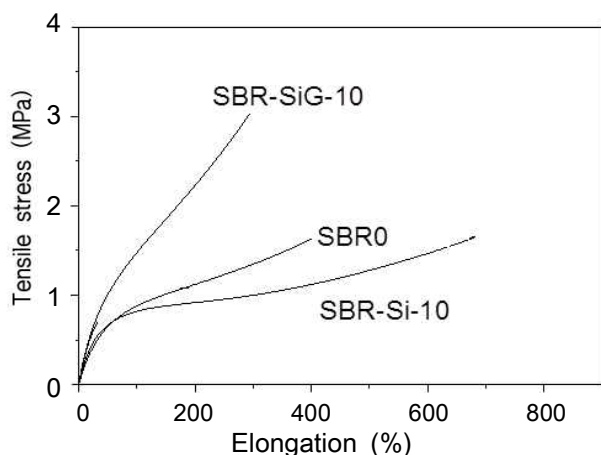


**Figure 6.** Stress-strain graph of gum and silica filled SBR vulcanizates

is calculated using the equations (2) and (3).

$$Q_r = \frac{\left[ \frac{m}{d_r} + \frac{(m_s - m)}{d_s} \right]}{m/d_r} \quad (2)$$

Where  $m$  and  $m_s$  are the rubber weights before and after swelling, respectively.  $d_r$  and  $d_s$  are the densities of rubber and toluene respectively.

$$\text{Swelling ratio} = Q_r/Q_0 \quad (3)$$

Where  $Q_r$ , equilibrium swelling value of silica filled vulcanizates,  $Q_0$  is the equilibrium swelling value of gum SBR vulcanizates. The equilibrium swelling ratio's decreases to about 14.6 % (10 phr) and 14.3 % (20 phr) on replacing silica particles with graphite coated silica samples (Silica-G). Similarly, equilibrium swelling ratio value decreases to about 12.2 % (10 phr) and 7.9 % (20 phr) on replacing silica particles with amorphous carbon coated silica samples (Si-AC) in SBR compounding formulations. Higher polymer-filler interaction between modified silica and SBR matrix resulted in the significant improvement in mechanical properties and reduction in swelling ratios.

### III. Conclusions:

Carbon coating on silica particles is done by grafting expanded graphite on the silica aggregates. Successful coating of carbon is corroborated using FT-IR, TGA, XPS and TEM. Crystalline nature of coated graphite is corroborated using XRD. Influence of carbon coated silica particles on rheological and mechanical properties of SBR composites are investigated. Carbon coated silica particles showed significant improvement in rheological and mechanical properties, when compared to pristine silica filled system corroborating higher polymer-filler adhesion. This fact was further supported by bound rubber content and equilibrium swelling ratios of unvulcanized and vulcanized SBR composites.

**Table 4.** Rheological results of Gum and silica filled SBR composites

| S. No | Samples    | Torques (lb-in) |       |                  | Scorch time, $t_{s2}$<br>(min) | Optimum cure time, $t_{90}$<br>(min) |
|-------|------------|-----------------|-------|------------------|--------------------------------|--------------------------------------|
|       |            | $M_L$           | $M_H$ | $DS = M_H - M_L$ |                                |                                      |
| 1.    | SBR0       | 2.0             | 19.5  | 17.5             | 04:26                          | 07:09                                |
| 2.    | SBR-Si-10  | 3.1             | 21.1  | 18.0             | 06:24                          | 13:18                                |
| 3.    | SBR-SSi-10 | 3.1             | 22.7  | 19.6             | 03:06                          | 06:21                                |
| 4.    | SBR-SiG-10 | 3.0             | 26.0  | 23.0             | 02:06                          | 06:27                                |
| 5.    | SBR-Si-20  | 8.0             | 35.0  | 27.0             | 05:14                          | 13:01                                |
| 6.    | SBR-SiG-20 | 5.0             | 32.0  | 27.0             | 01:02                          | 05:27                                |

**Table 5.** Mechanical properties and volume swelling of Gum and silica filled SBR composites

(Average of three samples are reported in the Table)

| S. No | Samples    | Modulus (MPa) | Tensile strength (MPa) | EB (%) | Equilibrium swelling ratio ( $Q_r/Q_0$ ) |
|-------|------------|---------------|------------------------|--------|--|
| 1.    | SBR0       | 1.06          | 1.76                   | 400    | 1.00                                     |
| 2.    | SBR-Si-10  | 1.15          | 1.65                   | 430    | 0.82                                     |
| 3.    | SBR-SSi-10 | 1.51          | 2.26                   | 490    | 0.78                                     |
| 4.    | SBR-SiG-10 | 1.94          | 3.19                   | 380    | 0.70                                     |
| 5.    | SBR-Si-20  | 1.62          | 2.35                   | 510    | 0.63                                     |
| 6.    | SBR-SiG-20 | 2.77          | 3.42                   | 300    | 0.54                                     |

### Acknowledgement

Authors thank to Korea Automotive Technology Institute for financial support.

### References

1. J. E. Mark, "*Science and Technology of Rubber*", Academic Press, San Diego, (1994).
2. K. A. Grosch, *Rubber Chem. Technol.*, **69**, 495 (1996).
3. B. Freund, F. Forster and R. Lotz, *Paper No. 77 presented at a meeting of ACS*, Rubber Division, Cleveland, Ohio, 17-20 October (1995).
4. J. W. ten brike, V. M. Litvinov, J. E. G. J. Wijnhoven, J. W. M. Noordermer, *Macromolecules*, **35**, 10026 (2002).
5. R. Mukhopadhyay, S. K. De, *Rubber Chem. Technol.*, **52**, 263 (1979).
6. S. Debnath, S. K. De, D. Khastgir, *J. Appl. Polym. Sci.*, **37**, 1449 (1989).
7. A. Mallick, D. K. Tripathy, S. K. De, *Rubber Chem. Technol.*, **67**, 845 (1994).
8. A. M. Shanmugharaj, Anil K. Bhowmick, *Rubber Chem. Technol.*, **75**, 605 (2002).
9. A. M. Shanmugharaj, Anil K. Bhowmick, *Rubber Chem. Technol.*, **76**, 299 (2003).
10. M. J. Wang, Y. Kutsovsky, P. Zhang, G. Mehos, L. J. Murphy, K. Mahmud, Presented at Functional tire fillers 2001, Fort Lauderdale, Florida, 29-31 January (2001).